Punjab University Journal of Mathematics (2025), 57(02), 180-200
https://doi.org/10.52280/pujm.2025.57(02)04

# Perturbation and Neural Network Approximation for flexible Blade Coating Analysis of Third Order Fluid with Lubrication Approximation Theory

*Saira Bhatti
Department of Mathematics, COMSATS University Islamabad, Abbottabad Campus, Abbottabad, Pakistan

Hunniya Sabir
Department of Mathematics, COMSATS University Islamabad, Abbottabad Campus, Abbottabad, Pakistan

Muhammad Zahid
Department of Mathematics, COMSATS University Islamabad, Abbottabad Campus, Abbottabad, Pakistan

Assad Ayub
Department of Mathematics and Statistics, Hazara University, Mansehra, Pakistan

Hafiz Abdul Wahab
Department of Mathematics and Statistics, Hazara University, Mansehra, Pakistan

*Corresponding Author
saira@cuiatd.edu.pk

Received: 18 February, 2025 / Accepted: 31 July, 2025 / Published online: 20 August, 2025

**Abstract.** The flexible blade coating process is widely used in various in-dustries for the production of thin films on substrates. However, the analy-sis of coating process for non-Newtonian fluids remains a challenging task due to their complex rheological behavior. In this work, we have used third order fluid along with flexible blade which is new and challenging because of the complexity of the non-linear equations, the surface being coated, decomposition of the functional material layers over complex geometries. The importance of our analysis is that it enables the optimization of the in-volved parameters which include gap height, blade angles, speed and most importantly fluid rheology. The perturbation approximation method with Levenberg–Marquardt neural network (LM–NN) is used to investigate the coating process of third order-fluids using lubrication approximation the-ory. The deformation of the blade during the coating process and behav-ior of fluid flow is represented in terms of system of nonlinear equations. Numerical solution has been obtained to analyze the blade flexibility and lubrication force on the coating process. For data training of LM–NN, 70 percent data is taken for training, 15 percent for validation and 15 per-cent data is used for testing. Our results show that the proposed method can accurately predict the coating thickness and the blade deformation for

different values of the coating parameters. Additionally, various physical parameters which influence the fluid motion like flexibility and speed of blade, including its rheological characteristics are graphically analyzed. The findings of the study suggest that a better understanding of the com-plex process of blade coating for non-Newtonian fluids can be explained through perturbation methods along with neural networks approximation, which can improve the coating process applications on industrial level.

**AMS (MOS) Subject Classification Codes: 70E20; 65M80; 68T07; 35Q30**
**Key Words:** Blade coating analysis, perturbation approximation with Neural networks, lubrication approximation theory, third order fluid.

## 1. INTRODUCTION

For the prevention of material corrosion and avoiding harmful atmospheric effects, coatings are considered to be very useful. Coatings are also useful for materials decoration by modifying material overall appearance, change in its color, polish and shining, and smoothness. Coating plays an important role in many industrial processes like modification of surface properties of a material, enhances its performance for the protection from corrosion and avoid degradation. Coatings are engineered in such a way that makes them beneficial for many industrial applications while conserving thermal stability optical transparency and electrical conductivity. The fluid industry has been revolutionized with coating, which enables the materials to maintain their properties in more challenging environments while increasing the lifespan and reducing the cost for its maintenance. Electronic and photovoltaic industries mostly rely upon the this process which controls the microstructures to produce high performance films.In order to design more efficient framework and to avoid waste of material, our analysis helps to understand the complex relationship between surface tension, material flow and substrate interaction. These aspects attracted the researchers and industrialists towards various applications of blade coating process and built a linkage between industry and the university. Blade coating along with flexibility is very important in various coating industries but this technique faces several limitations, including achieving uniformly thin films, handling different ranges of viscosities and managing particles of large sizes. Furthermore, blade clogging, defects in surface and setup complexities can reduce the effectiveness of the work.

In order to address the key challenges in engineering and industry, recent research have combined bioinspired and hybrid approaches. In this regard, a pioneer work related to the blade coating flows has been presented by many authors [20,8,4] for Newtonian fluids. Middleman [14] work and Ruschak [17] article described the process of blade coating. The connection between coat weight and the angle of blade was elucidated by Booth [3]. The Hwang [12] introduced power law fluid in the plane blade coater and introduced approximate flow solution. Dien and Elord [6] obtained the numerical solution of power law fluid. Greener and Middleman [10] analyzed the viscoelastic fluid by using power law in roll coating. Later on, Savage [19] fixed the errors created by Greener and Middleman [10]. Moreover, Ross et al. [16] used the plane coater to examine the behavior of power-law fluid and analyzed that the pressure distribution and blade load increased or decreased, in

the form of weak non-Newtonian fluid nature, depending on height ratio and blade shape of the coater then Newtonian fluid values. Sinha and Singh [22] examined the model of the roll coating for power law fluid. Furthermore, Corvalan and Saita [5] presented the deformation of compressible substrate by using the finite element method. Sajid et al. [18] analyzed that when the non-Newtonian parameters increased, then the pressure which was present in the region of flow also increased, while the geometry of the flow was totally distinct. For rigid blade coating, Siddiqui et al. [21] presented the mathematical model for Williamson fluid. Lubrication approximation theory (LAT) was used to examine the coating properties by Ali et al. [1] in which he calculated the properties of the fluid flow under a different geometry of coating with same complex fluids and obtained the same physical conclusions. Maxwell model of flow in blade coating was studied by Tichy [23] who evaluated that the pressure can be decreased or increased by viscoelastic effects. Hsu et al.

In [11] authors separated viscoelastic fluid and Newtonian forces in blade, which lubrication theory was used, and then the results were experimentally and theoretically compared. Rana et al [15] studied the blade coating process for Powel-Eyring fluid using LAT analysis. Some more work on blade coating analysis using non-Newtonian fluid has been studied by Bhatti et al [2]. Since we are using flexible blade in our study, some work related to flexible blade coater has been modelled and studied in [9, 13, 25]. Previously blade coating for third order fluid with fixed blade has been studied by Bhatti et al. [2]. In order to enhance the importance of this work from an industrial point of view, modelling for the flexible blade is used and observed mathematically that the blade coating can be controlled by increasing or decreasing the non- Newtonian parameter. The flexibility of the blade is also very important for controlling the coating thickness. It means that coating of desired thickness can be obtained and controlled by controlling the flexibility of the blade.

In order to study the fluids flow in confined spaces, the Lubrication approximation theory (LAT) is an excellent mathematical tool for simplification of fluid flow in thin geometries. This theory is related to geometries which involve narrow gaps, for example, bearings which have moving surfaces with narrow gaps, micro channels and thin film coatings. Under small aspect ratio and low Reynolds number assumptions, the Navier Stokes equations are utilized for the derivation of simplified equations. It is assumed that the fluid film is thinner than that of the confining surfaces, which lead us to constitute simplified equations fluid flow which describes a balance between viscous stresses and pressure forces [26]. Thus, in our analysis of the process of blade coating, LAT has been employed for modeling the non-Newtonian fluid flow between the blade and the substrate. Since the lubrication forces are present between the fluid film and the blade, we can utilize LAT to provide significant understandings of the coating thickness and blade deformation.

In present research, the coating process of third order fluid has been investigated by applying LAT by considering a flexible blade. The constitutive equations for motion which describe the blade deformation and fluid motion are detailed in terms of a system of nonlinear differential equations. The solution of these equations has been obtained by a finite difference scheme. The obtained results clearly state that the LAT predicts the blade deformation and coating thickness accurately for different coating parameter values. The findings of the study suggest that a better understanding of the complex process of blade coating for non-Newtonian fluids can be explained through perturbation methods along

with neural networks approximation, which can improve the coating process applications on industrial level.

Perturbation approximation is a mathematical technique used to approximate the solution to complex equations that cannot be solved exactly. This technique involves breaking down the complex equation into simpler equations and then using a series expansion to find an approximate solution [7, 24]. Perturbation approximation is widely used in various fields of science and engineering, such as fluid mechanics, quantum mechanics, and nonlinear dynamics. In this paper a perturbation approximation method is used to analyze the coating process of third order fluids using lubrication approximation theory. The proposed method provides a new approach to analyzing the coating process of non-Newtonian fluids, which can be challenging due to their complex rheological behavior. By applying perturbation approximation, we can obtain an approximate solution to the equations that govern the coating process of non-Newtonian fluids, which can be used to optimize the process for various industrial applications.

## 2. Problem Formulation and Constitutive Equations

The constitutive equations for continuity and momentum for an incompressible viscous fluid flow and without the presence of body forces are given as under [2]:

$$\nabla.\overrightarrow{V} = 0, \tag{2. 1}$$

$$\rho\frac{D\overrightarrow{V}}{Dt} = -\nabla \mathrm{P} + \mathrm{div}\tau, \tag{2. 2}$$

where $\overrightarrow{V}$, represents the velocity profile, Pressure is denoted by $\mathrm{P}$ , $\tau$ represents the Cauchy stress tensor, constant fluid density is represented by $\rho$,and $\frac{D}{Dt}$ represents the material derivative and we can also write it as

$$\frac{D\overrightarrow{V}}{Dt} = \frac{\partial\overrightarrow{V}}{\partial t} + \left(\overrightarrow{V}.\nabla\right)\overrightarrow{V} \tag{2. 3}$$

## 3. Constitutive Equations

The extra stress tensor $\tau$ for third order fluid [2] is given as under:

$$\tau = \mu\overrightarrow{A}_1 + \alpha_1\overrightarrow{A}_2 + \alpha_2\overrightarrow{A}_1{}^2 + \gamma_1\overrightarrow{A}_3 + \gamma_2\left(\overrightarrow{A}_1\overrightarrow{A}_2 + \overrightarrow{A}_2\overrightarrow{A}_1\right) + \gamma_3\left(tr\left(\overrightarrow{A}_1{}^2\right)\right)\overrightarrow{A}_1, \tag{3. 4}$$

where $\mu$ is the viscosity,$\alpha_1$ is the plasticity and $\alpha_2$ is the cross viscosity, $\gamma_1, \gamma_2, \gamma_3$ are material parameters and Rivlin-Ericksen tensors are represented by $\overrightarrow{A}_1$, $\overrightarrow{A}_2$, $\overrightarrow{A}_3$ and are defined as follows:

$$\overrightarrow{A}_1 = \nabla\overrightarrow{V} + \left(\nabla\overrightarrow{V}\right)^T, \tag{3. 5}$$

$$\overrightarrow{A}_2 = \frac{d}{dt}\overrightarrow{A}_1 + \overrightarrow{A}_1\left(\nabla\overrightarrow{V}\right) + \left(\nabla\overrightarrow{V}\right)^T\overrightarrow{A}_1, \tag{3. 6}$$

$$\overrightarrow{A}_3 = \frac{d}{dt}\overrightarrow{A}_2 + \overrightarrow{A}_2\left(\nabla\overrightarrow{V}\right) + \left(\nabla\overrightarrow{V}\right)^T\overrightarrow{A}_2. \tag{3. 7}$$

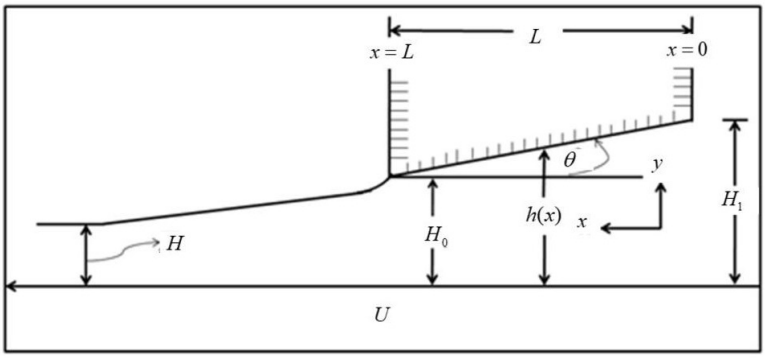


FIGURE 1. Geometry of the problem

## 4. STATEMENT AND THE GEOMETRY OF THE PROBLEM

The Fig. 1 represents a two-dimensional incompressible, isothermal and steady fluid flow in flexible blade coa ter and is given in Cartesian coordinate system. The distribution of the pressure loads the blade and as a result it deflects. The angle $\theta$ is taken as the web angle constructed by the chord of $L$ length which connects the edges having height $y = H_1$ and $y = H_0$. At $y = h(x)$, the blade is kept flexible at an angle $\sin\theta = \frac{H_1 - H_0}{L}$. The moving blade has length $L$, while the one edge of the blade at $x = 0$ with height $H_1$ and the other edge at $x = L$ with height $H_0$. It is supposed that the LAT in the flow field is effective. Figure 1 is given for detailed description.

## 5. APPLICATION OF LUBRICATION APPROXIMATION METHOD LAT

We initiate from the geometry of the problem with the LAT analysis and note that the principal dynamical event is occurring in the nip of the blade. Since the distance between blade and substrate is small at the nip as compared to the length of substrate, which is negligible. Here fluid motion is considered in $x$-direction due to the fact that motion in $y$-axis is small. Subsequently, it is appropriate to suppose that $v \ll u$ and $\frac{\partial}{\partial x} \ll \frac{\partial}{\partial y}$, as a result Eq. (2. 1) becomes, $\frac{\partial u}{\partial x} = 0$, and here the velocity profile turns out $\overrightarrow{V} = [u(y),\ 0]$. The equation of continuity is satisfied.

Momentum equation in x-component is

$$\rho\left(u\frac{\partial u}{\partial x} + v\frac{\partial u}{\partial y}\right) = -\frac{\partial p}{\partial x} + \frac{\partial \tau_{xx}}{\partial x} + \frac{\partial \tau_{xy}}{\partial y}. \tag{5. 8}$$

Momentum equation in $y$-component is

$$\rho\left(u\frac{\partial v}{\partial x} + v\frac{\partial v}{\partial y}\right) = -\frac{\partial p}{\partial y} + \frac{\partial \tau_{yx}}{\partial x} + \frac{\partial \tau_{yy}}{\partial y}. \tag{5. 9}$$

Since $\frac{\partial}{\partial x} \ll \frac{\partial}{\partial y,}$ and $\overrightarrow{V} = [u(y),\ 0]$, which implies that $\frac{\partial u}{\partial x} = 0$, so in the momentum equation, the acceleration part disappears and on $x$-component the Eq. (5. 8) becomes

$$-\frac{\partial p}{\partial x} + \frac{d\tau_{xy}}{dy} = 0, \tag{5. 10}$$

and $y$-component Eq. (5. 9) takes the form

$$-\frac{\partial p}{\partial y}+\frac{d\tau_{yy}}{dy}=0. \tag{5. 11}$$

Using components of shear stress

$$\tau_{xy}=\tau_{yx}=\mu\frac{du}{dy}+2(\gamma_2+\frac{\gamma_3}{2})\left(\frac{du}{dy}\right)^3, \tag{5. 12}$$

$$\tau_{yy}=(2\alpha_1+\alpha_2)\left(\frac{du}{dy}\right)^2. \tag{5. 13}$$

The generalized pressure P is given as follows:

$$P(x,y) \;=\; p(x,y)-(2\alpha_1+\alpha_2)\left(\frac{du}{dy}\right)^2. \tag{5. 14}$$

Now making use of the Eq. (5. 12) and the Eq. (5. 13) into the Eq. (5. 10), we arrive at

$$\mu\frac{d^2u}{dy^2}+2\left(\gamma_2+\frac{\gamma_3}{2}\right)\frac{d}{dy}\left(\frac{du}{dy}\right)^3=\frac{\partial P}{\partial x}\,. \tag{5. 15}$$

Making use of the Eq. (5. 13) and the Eq. (5. 14) into the Eq. (5. 11), then it becomes

$$\frac{\partial P}{\partial y}=0. \tag{5. 16}$$

The Eq. (5. 16) describes that pressure $P$ depends on coordinate $x$ only. Thus, by placing $\gamma=\gamma_2+\frac{\gamma_3}{2},$ Eq. (5. 15) becomes

$$\mu\frac{d^2u}{dy^2}+2\gamma\frac{d}{dy}\left(\frac{du}{dy}\right)^3=\frac{dP}{dx}. \tag{5. 17}$$

The Eq. (5. 17) will be studied subject to the following boundary conditions:

$$u=\begin{cases} U & at\ y=0,\\ 0 & at\ y=h(x)\,. \end{cases} \tag{5. 18}$$

## 6. NON-DIMENSIONAL FORM

In order to write the nonlinear differential equation given in Eq. (5. 17) and boundary conditions given in Eq. (5. 18) in dimensionless form, we consider the following assumptions:

$$x^*=\frac{x}{L}\,,\ y^*=\frac{y}{L}\,,\ u^*=\frac{u}{U}\,,\ P^*=\frac{p{H_0}^2}{\mu UL}\,,\ \tilde{h}=\frac{h}{H_0}\,,\ \gamma^*=\frac{U^2\gamma}{\mu H_0}\,,\ \lambda=\frac{Q}{UWH_0}\,. \tag{6. 19}$$

Using these parameters in Eq. (5. 17) and finally, after neglecting the asterisk sign the Eq. (5. 17) becomes

$$\frac{d^2u}{dy^2}+2\gamma\frac{d}{dy}\left(\frac{du}{dy}\right)^3=\frac{dP}{dx}\,. \tag{6. 20}$$

On integrating the Eq. (6. 20) we have

$$\frac{du}{dy}+2\gamma\left(\frac{du}{dy}\right)^3=\frac{dP}{dx}y+C. \tag{6. 21}$$

In the above equation, $C$ is known as constant of integration that depends on the $\gamma$. By using required assumptions, the dimensionless form of the boundary conditions is given a follows:

$$u = \begin{cases} 1 & if \quad y = 0, \\ 0 & if \quad y = \tilde{h}\,(x)\,. \end{cases} \tag{6. 22}$$

It should be noted that for flexible blade coater $\tilde{h}(x) = \beta - \frac{\beta(k-1)(x)}{k}$, and $k = \frac{H_1}{H_0}$.

## 7. Flow rate

The volumetric flow rate per unit width can be calculated by using following formula,

$$\frac{Q}{W} = \int_0^h u\, dy. \tag{7. 23}$$

The width of web is $W$. The dimensionless final coating thickness is,

$$\lambda = \int_0^{\tilde{h}} u\, dy. \tag{7. 24}$$

## 8. Problem Solution

To solve the Eq. (6. 21) along with Eq. (6. 22), we have used the perturbation method because this equation is non-linear and difficult to solve exactly. This method relies on the small parameter which is present in the problem to be perturbed for approximation. Let us consider $\gamma \ll 1$, and then we expand.

$$\left.\begin{array}{c} u = u_0 + \gamma u_1, \\ p = p_0 + \gamma p_1, \\ C = C_0 + \gamma C_1, \\ \lambda = \lambda_0 + \gamma \lambda_1, \\ \frac{dp}{dx} = \frac{dp_0}{dx} + \gamma \frac{dp_1.}{dx} \end{array}\right] \tag{8. 25}$$

By using the values of Eq. (8. 25) into the Eq. (6. 21) and Eq. (6. 22) and then comparing the same powers of $\gamma$, the following problems are acquired.

8.1. **The problem of order zero.** The problem of order zero is obtained by equating the terms without $\gamma$ which is given as,

$$\frac{du_0}{dy} = \frac{dp_0}{dx} y + C_0. \tag{8. 26}$$

The boundary conditions for zero-order becomes,

$$\left.\begin{array}{rl} u_0 = 1 & \text{when } \ y = 0, \\ u_0 = 0 & \text{when } y = \tilde{h}\,(x)\,. \end{array}\right\} \tag{8. 27}$$

The volumetric flow rate for zero-order becomes,

$$\lambda_0 = \int_0^{\tilde{h}} u_0\, dy. \tag{8. 28}$$

The solution of the zeroth order velocity profile using the boundary condition is,

$$u_0 = \frac{1}{2}\frac{dp_0}{dx}\left(y^2 - \tilde{h}y\right) - \frac{y}{\tilde{h}} + 1. \tag{8. 29}$$

This solution is the same as obtained by Middleman [4]. Using Eq. (8. 29) in Eq. (8. 28), integrating and simplification gives

$$\lambda_0 = \left( -\frac{1}{12}\frac{dp_0}{dx}\tilde{h}^3 + \frac{\tilde{h}}{2} \right). \tag{8. 30}$$

This gives us the zero-order pressure gradient.

$$\frac{dp_0}{dx} = \frac{6}{\tilde{h}^2} - \frac{12}{\tilde{h}^3}\lambda_0. \tag{8. 31}$$

By using $\tilde{h}\,(x) = \beta - \frac{\beta(k-1)(x)}{k}$ in Eq. (8. 31) we have

$$\frac{dp_0}{dx} = \frac{6}{\left(\beta - \frac{\beta(k-1)(x)}{k}\right)^2} - \frac{12}{\left(\beta - \frac{\beta(k-1)(x)}{k}\right)^3}\lambda_0. \tag{8. 32}$$

On integrating the above equation, we have

$$p_0 = \frac{6k}{\left(\beta - \frac{\beta(k-1)(x)}{k}\right)\beta\,(k-1)} - \frac{6k\lambda_0}{\left(\beta - \frac{\beta(k-1)(x)}{k}\right)^2\beta\,(k-1)} + C\,. \tag{8. 33}$$

At the entrance and exit of the blade, we take pressure equal to zero,

$$p_0\,(0) = 0,\;\; p_0\,(1) = 0. \tag{8. 34}$$

After simplifying we get,

$$\lambda_0 = \frac{\beta}{(k+1)}. \tag{8. 35}$$

By using the boundary conditions and after simplification,

$$p_0 = \frac{6k^2\tilde{h}\beta\,(k+1) - 6\lambda_0 k\beta\,(k-1) - 6k^2\tilde{h}^2}{\tilde{h}^2\beta^2\,(k^2-1)}\,. \tag{8. 36}$$

8.2. **The problem of order one.** The problem of order one is given as,

$$\frac{du_1}{dy} + 2\left(\frac{du_0}{dy}\right)^3 = \frac{dp_1}{dx}y + C_1. \tag{8. 37}$$

The boundary conditions for first-order problem become,

$$\left.\begin{array}{rr} u_1 = 0 & \text{if } \; y = 0, \\ u_1 = 0 & \text{if } y = \tilde{h}\,(x)\,. \end{array}\right\} \tag{8. 38}$$

The volumetric flow rate for first order becomes,

$$\lambda_1 = \int_0^{\tilde{h}} u_1\, dy. \tag{8. 39}$$

After solving the Eq. (8. 37) along with the boundary conditions, the velocity of first order becomes,

$$\begin{aligned} u_1 = \tfrac{1}{2}\tfrac{dp_1}{dx}\left(y^2-\tilde{h}y\right) - \tfrac{1}{2}\left(\tfrac{dp_0}{dx}\right)^3\left(y^4-\tilde{h}^3y\right) \\ +\tfrac{1}{3}\left(y^3-\tilde{h}^2y\right)\left(3h\left(\tfrac{dp_0}{dx}\right)^3+\tfrac{6}{\tilde{h}}\left(\tfrac{dp_0}{dx}\right)^2\right) \\ -\left(\tfrac{3}{4}\tilde{h}^2\left(\tfrac{dp_0}{dx}\right)^3+3\left(\tfrac{dp_0}{dx}\right)^2+\tfrac{3}{\tilde{h}^2}\left(\tfrac{dp_0}{dx}\right)\right)\left(y^2-\tilde{h}y\right). \end{aligned} \tag{8. 40}$$

After solving, Eq. (8. 39) becomes,

$$\lambda_1 = -\frac{\tilde{h}^3}{12}\left(\frac{dp_1}{dx}\right)+\frac{\tilde{h}^5}{40}\left(\frac{dp_0}{dx}\right)^3+\frac{\tilde{h}}{2}\left(\frac{dp_0}{dx}\right). \tag{8. 41}$$

Now by separating $\frac{dp_1}{dx}$, from Eq. (8. 41) we have,

$$\frac{dp_1}{dx} = \frac{3\tilde{h}^2}{10}\left(\frac{dp_0}{dx}\right)^3+\frac{6}{\tilde{h}^2}\left(\frac{dp_0}{dx}\right)-\frac{12\lambda_1}{\tilde{h}^3}\ . \tag{8. 42}$$

By using Eq. (8. 32) in Eq. (8. 42) we have,

$$\frac{dp_1}{dx} = \frac{3\tilde{h}^2}{10}\left(\frac{6}{\tilde{h}^2}-\frac{12}{\tilde{h}^3}\lambda_0\right)^3+\frac{6}{\tilde{h}^2}\left(\frac{6}{\tilde{h}^2}-\frac{12}{\tilde{h}^3}\lambda_0\right)-\frac{12\lambda_1}{\tilde{h}^3}\ . \tag{8. 43}$$

Finally, the first-order pressure gradient becomes,

$$\frac{dp_1}{dx} = \frac{504}{5\tilde{h}^4}-\frac{2304\lambda_0}{5\tilde{h}^5}+\frac{3888{\lambda_0}^2}{5\tilde{h}^6}-\frac{2592{\lambda_0}^3}{5\tilde{h}^7}-\frac{12\lambda_1}{\tilde{h}^3}\ . \tag{8. 44}$$

Now by using $\tilde{h}\,(x) = \beta - \frac{\beta(k-1)(x)}{k}$, Eq. (8. 44) we have

$$\begin{aligned} \tfrac{dp_1}{dx} = \tfrac{504\left(\beta-\frac{\beta(k-1)(x)}{k}\right)^{-4}}{5} - \tfrac{2304\lambda_0\left(\beta-\frac{\beta(k-1)(x)}{k}\right)^{-5}}{5} + \tfrac{3888{\lambda_0}^2\left(\beta-\frac{\beta(k-1)(x)}{k}\right)^{-6}}{5} \\ -\tfrac{2592{\lambda_0}^3\left(\beta-\frac{\beta(k-1)(x)}{k}\right)^{-7}}{5} - 12\lambda_1\left(\beta-\tfrac{\beta(k-1)(x)}{k}\right)^{-3}\ . \end{aligned} \tag{8. 45}$$

After integrating Eq. (8. 45) we get,

$$\begin{aligned} p_1 = \tfrac{168k\left(\beta-\frac{\beta(k-1)(x)}{k}\right)^{-3}}{5\beta(k-1)} - \tfrac{576k\lambda_0\left(\beta-\frac{\beta(k-1)(x)}{k}\right)^{-4}}{5\beta(k-1)} \\ +\tfrac{3888k{\lambda_0}^2\left(\beta-\frac{\beta(k-1)(x)}{k}\right)^{-5}}{25\beta(k-1)} - \tfrac{432k{\lambda_0}^3\left(\beta-\frac{\beta(k-1)(x)}{k}\right)^{-6}}{5\beta(k-1)} \\ -\tfrac{6k\lambda_1}{\beta(k-1)}\left(\beta-\tfrac{\beta(k-1)(x)}{k}\right)^{-2}+C. \end{aligned} \tag{8. 46}$$

At the entrance and exit of the blade we take pressure equal to zero,

$$p_1\,(0) = 0,\ \ p_1\,(1) = 0. \tag{8. 47}$$

$$\begin{aligned} \lambda_1 = \tfrac{28\left(k^2+k+1\right)}{5\beta(k+1)} - \tfrac{96\lambda_0\left(k^2+1\right)}{5\beta^2} + \tfrac{648{\lambda_0}^2\left(k^3+k+\frac{1}{k+1}\right)}{25\beta^3} \\ -\tfrac{72{\lambda_0}^3\left(k^4+k^2+1\right)}{5\beta^4}\ . \end{aligned} \tag{8. 48}$$

After using boundary conditions in Eq. (8. 46) first-order pressure becomes,

$$\begin{array}{c} p_1 = \frac{168k\left(\beta-\frac{\beta(k-1)(x)}{k}\right)^{-3}}{5\beta(k-1)} - \frac{576k\lambda_0\left(\beta-\frac{\beta(k-1)(x)}{k}\right)^{-4}}{5\beta(k-1)} \\ +\frac{3888k{\lambda_0}^2\left(\beta-\frac{\beta(k-1)(x)}{k}\right)^{-5}}{25\beta(k-1)} - \frac{432k{\lambda_0}^3\left(\beta-\frac{\beta(k-1)(x)}{k}\right)^{-6}}{5\beta(k-1)} \\ -\frac{6k\lambda_1}{\beta(k-1)}\left(\beta-\frac{\beta(k-1)(x)}{k}\right)^{-2} + \frac{6k}{5\beta^3(k-1)}\left(\begin{array}{c}\left(-\frac{28}{\beta}+\frac{96\lambda_0}{\beta^2}-\frac{648{\lambda_0}^2}{5\beta^3}\right)\\ +\frac{72{\lambda_0}^3}{\beta^4}+5\lambda_1\end{array}\right). \end{array} \tag{8. 49}$$

By using $\tilde{h} = \beta - \frac{\beta(k-1)(x)}{k}$ in Eq. (8. 49) we get the expression for first-order pressure,

$$\begin{array}{c} p_1 = \frac{168k}{5\tilde{h}^3(k-1)\beta} - \frac{576k\lambda_0}{5\tilde{h}^4(k-1)\beta} + \frac{3888k{\lambda_0}^2}{25\tilde{h}^5(k-1)\beta} - \frac{432k{\lambda_0}^3}{5\beta(k-1)\tilde{h}^6} \\ -\frac{6k\lambda_1}{\beta(k-1)\tilde{h}^2} + \frac{6k}{5(k-1)\beta^3}\left(-\frac{28}{\beta}+\frac{96\lambda_0}{\beta^2}-\frac{648{\lambda_0}^2}{5\beta^3}+\frac{72{\lambda_0}^3}{\beta^4}+5\lambda_1\right). \end{array} \tag{8. 50}$$

Thus, the approximate solution up to first order can be obtained as follows;

$$u = u_0 + \gamma u_1. \tag{8. 51}$$

Making use of the Eq. (8. 29) and Eq. (8. 30) into the Eq. (8. 51), the velocity up to the first order is,

$$\begin{array}{l} u = \left(\frac{1}{2}\frac{dp_0}{dx}\left(y^2-\tilde{h}y\right)-\frac{y}{\tilde{h}}+1\right) \\ +\gamma\left(\begin{array}{c} \frac{1}{2}\frac{dp_1}{dx}\left(y^2-\tilde{h}y\right)-\frac{1}{2}\left(\frac{dp_0}{dx}\right)^3\left(y^4-\tilde{h}^3y\right) \\ +\frac{1}{3}\left(y^3-\tilde{h}^2y\right)\left(3\tilde{h}\left(\frac{dp_0}{dx}\right)^3+\frac{6}{\tilde{h}}\left(\frac{dp_0}{dx}\right)^2\right) \\ -\left(\frac{3}{4}\tilde{h}^2\left(\frac{dp_0}{dx}\right)^3+3\left(\frac{dp_0}{dx}\right)^2+\frac{3}{\tilde{h}^2}\left(\frac{dp_0}{dx}\right)\right)\left(y^2-\tilde{h}y\right) \end{array}\right). \end{array} \tag{8. 52}$$

Pressure gradient up to first order is given as,

$$\frac{dp}{dx} = \frac{dp_0}{dx} + \gamma\frac{dp_1}{dx}. \tag{8. 53}$$

Putting the Eq. (8. 32) and the Eq. (8. 41) into the Eq. (8. 53) we get,

$$\begin{array}{c} \frac{dp}{dx} = \left(\frac{6}{\tilde{h}^2}-\frac{12}{\tilde{h}^3}\lambda_0\right) \\ +\gamma\left(\frac{504}{5\tilde{h}^4}-\frac{2304\lambda_0}{5\tilde{h}^5}+\frac{3888{\lambda_0}^2}{5\tilde{h}^6}-\frac{2592{\lambda_0}^3}{5\tilde{h}^7}-\frac{12\lambda_1}{\tilde{h}^3}\right). \end{array} \tag{8. 54}$$

The flow rate up to first order is given as below,

$$\lambda = \lambda_0 + \gamma\lambda_1, \tag{8. 55}$$

Using the Eq. (8. 35) and Eq. (8. 48) into the Eq. (8. 55), we have,

$$\lambda = \left(\frac{\beta}{(k+1)}\right) + \gamma\left(\begin{array}{c}\frac{28\left(k^2+k+1\right)}{5\beta(k+1)}-\frac{96\lambda_0\left(k^2-1\right)}{5\beta^2}\\ +\frac{648{\lambda_0}^2\left(k^3+k+\frac{1}{k+1}\right)}{5\beta^3}-\frac{72{\lambda_0}^3\left(k^4+k^2+1\right)}{5\beta^4}\end{array}\right). \tag{8. 56}$$

Pressure up to first order is given as,

$$p = p_0 + \gamma p_1. \tag{8. 57}$$

We use the Eq. (8. 36) and Eq. (8. 46) into the Eq. (8. 57), to get,

$$p = \left(\frac{6k}{\bar{h}\beta(k-1)} - \frac{6k\lambda_0}{\bar{h}^2\beta(k-1)} - \frac{6k^2}{\beta^2(k^2-1)}\right) + \gamma\left(\begin{array}{c} \frac{168k}{5\bar{h}^3(k-1)\beta} - \frac{576k\lambda_0}{5\bar{h}^4(k-1)\beta} + \frac{3888k{\lambda_0}^2}{25\bar{h}^5(k-1)\beta} - \frac{432k{\lambda_0}^3}{5\beta\bar{h}^6(k-1)} - \frac{6k\lambda_1}{\beta\bar{h}^2(k-1)} \\ + \frac{6k}{5\beta^3(k-1)}\left(-\frac{28}{\beta} + \frac{96\lambda_0}{\beta^2} - \frac{648{\lambda_0}^2}{5\beta^3} + \frac{72{\lambda_0}^3}{\beta^4} + 5\lambda_1\right) \end{array}\right). \tag{8. 58}$$

## 9. Operating Variables

After finding the velocity, pressure distribution, and pressure gradient all the captivating engineering quantities are easily accessible. We compute the operating variables in the given way.

9.1. **Blade Loading.** The pressure distribution loads the blade and makes it deflect. When the blade is flexible, then the blade loading $L$ can be calculated as

$$L = \int_0^1 p dx. \tag{9. 59}$$

We use the Eq. (8. 58) into the Eq. (9. 59) to get,

$$L = \int_0^1 \left( + \gamma \left( \begin{array}{c} \left(\frac{6k}{\bar{h}\beta(k-1)} - \frac{6k\lambda_0}{\bar{h}^2\beta(k-1)} - \frac{6k^2}{\beta^2(k^2-1)}\right) \\ \frac{168k}{5(k-1)\beta\bar{h}^3} - \frac{576k\lambda_0}{5\bar{h}^4\beta(k-1)} + \frac{3888k{\lambda_0}^2}{25\bar{h}^5\beta(k-1)} \\ - \frac{432k{\lambda_0}^3}{5(k-1)\beta\bar{h}^6} - \frac{6k\lambda_1}{(k-1)\beta\bar{h}^2} \\ + \frac{6k}{5\beta^3(k-1)}\left(-\frac{28}{\beta} + \frac{96\lambda_0}{\beta^2} - \frac{648{\lambda_0}^2}{5\beta^3} + \frac{72{\lambda_0}^3}{\beta^4} + 5\lambda_1\right) \end{array} \right) \right) dx. \tag{9. 60}$$

## 10. Results and Discussion

In this paper, the theoretical study of the blade coating analysis for viscous fluid has been studied using flexible blade. For the simplification of resultant equations, LAT is applied. To find the theoretical result perturbation method has been used while some of the results have been computed numerically.

Figs. 2 (a - f) represent the velocity profile for various values of non-Newtonian parameter $\gamma$ at different positions of the blade. In this case calculated validation checks are 1.9104e-07 at 142 epochs, error histogram is 0.000173 at with 20 bins, gradient is 2.7567e-05, Mu is 1e-10 and validation checks are 6 at 148 epochs.

For the validation of data set which the network achieved, the BVP represents the lowest error. This value physically interprets how accurately the network generalized the unseen data with high accuracy. The neural network suggests weights, architecture and algorithms are well defined. The error histogram physically represents the error distribution for actual target and predicted output. For spread and symmetry interpretation and observation of whether the model is skewed, biases of making big errors in some defined ranges, the error values are divided into 20 ranges (20 bins). The performance slop function is referred by the gradient with respect to the weights. The small value of gradient (2.7567e-05) means that the training has approached a minimum and no more changes in weights are

required, since it will be negligible. To control the update size of weights, the damping parameter Mu has been used. The very small value of Mu refers to an algorithm with Gauss-Newton behaviour, while a smaller value of damping parameter Mu reflects that the model has achieved its convergence and only fine tuned adjustments are needed at this stage. The lowest valid error has been achieved by the model for its best performance, which is shown by an epoch (one complete cycle through the entire dataset training). The physical interpretation of ANN parameters is given as under.

**Validation checks:** Overfitting warning: training stops if error doesn't improve.
**Calculated validation:** During training, the best validation error has been achieved
**Error Histogram:** Error spread representation: narrow with low peak error is presented here.
**Gradient:** Refers to how the error surface is steep; convergence= small gradient
**Mu:** A damping parameter
**Epochs:** Training iterations; critical to assess generalization and learning.

Whereas the Figs. 3 (a - f) have been sketched for various values of flexible parameter $\beta$ at different positions of the blade. It has been noticed that the fluid velocity decreases by increasing the value of the non-Newtonian parameters. According to physical perspective, an increase in value of $\gamma$ correlates to shear thickening effects, which increases the fluid viscosity and decreases the fluid velocity. From these figures it is observed that with increasing $\gamma$, the non-Newtonian character also increases, which increases shear thickening and causes the reduction in the fluid velocity, while by increasing the value of $\beta$, the velocity of the fluid increases means if the blade is more flexible velocity of fluid is more, while for less flexible blade velocity is also less physically it means that with more flexibility more fluid can pass from the gap while if the blade is less flexible velocity of the fluid is less so less fluid will pass from the gap. In this case calculated validation performance are 1.022e-07 at 1000 epochs, error histogram is 4.43e-05 at with 20 bins, gradient is 4.1156e-07, Mu is 1e-9 and validation checks are 0 at same number of epochs.

Hence in this analysis, the best performance has been achieved by the artificial neural network which signifies an extremely low generalization error. On the unseen data, the excellent predictive accuracy also achieved. The error histogram suggests unbiased and consistent output across different samples because most prediction errors lie in a very narrow range. A concisely small value of gradient value shows that the performance of the network surface has nearly been flattened. Thus, the model is very close to a global or local minimum error function. The damping factor Mu confirms that the training algorithm has been transitioned into fine-tuning mode. More precisely, it can be concluded that these parameters describe a well-generalized, optimally trained and highly stable model of neural network.

Pressure for various values of $\beta$ is depicted in Fig. 4(a - d), while pressure for various values of $\gamma$ is depicted in Fig. 5(a - d). It is observed that the pressure increases with increasing $\gamma$, so we concluded that pressure is more for non-Newtonian fluid as compared to Newtonian fluids, because by increasing the non-Newtonian parameter shear thickening increases which inserts more pressure. From Fig. 4(a - d) it is clear that pressure decreases by increasing the value of $\beta$, it means that by increasing the value of flexible parameter there is more gap between the blade and the substrate so fluid can easily pass through this

gap and hence exerts less pressure. In this case calculated validation performances are 3.8283e-07 at 84 epochs, error histogram is 0.000485 at with 20 bins, gradient is 8.4995e-05, Mu is 1e-10 and validation checks are 6 at 90 epochs.
It is clear from the basic rheology that $\gamma$ is related to shear thickening Figs. 5(a - d). Therefore, an increase in $\gamma$ will lead to higher effective viscosity, higher pressure and lower velocity. On the other hand, $\beta$ is related to the deformation. Higher $\beta$ means that there is wider area available for the fluid flow which perpetuates less pressure drop and higher velocity rates. In this case calculated validation performances are 1.0683e-07 at 169 epochs, error histogram is 0.000224 at with 20 bins, gradient is 6.3335e-06, Mu is 1e-8 and validation checks are 6 at 175 epochs.
All the results in the given paper from Figs. 2(a - f) to Figs. 5(a - d) and from Table 1 to Table 4 can be deduced from the given discussion. Figs. (6 – 9) are statistical graphs of physical analysis of numerical values tabulated in Table 4 and Table 5.

Table 1 and Table 2 show numerical values of solution including Epoch, elapsed time, performance, gradient and $\mu$ for velocity and pressure distribution simultaneously.

Table 3 shows that the non-Newtonian parameter effects on the coating thickness and blade loading. It is worth mentioning to observe that by increasing the non-Newtonian parameter values, the blade loading increases, and coating thickness also increases. So more non-Newtonian fluid will exert more load compared to Newtonian fluid and the coating thickness for non-Newtonian fluid is more as compared to Newtonian fluid. While Table 4 shows the effect of flexibility parameter on coating thickness and blade loading, it is clear from the table that blade loading decreases by increasing the flexibility parameter, and coating thickness increases by increasing the flexibility parameter, it means more flexible blade will reduce the blade loading and increase the coating thickness. We can control the blade loading and coating thickness by changing these parameters and can get thickness of the desired requirement. Figure 6-9 are there to present the pictorial representation of tabular data.

For different values of the parameters $\alpha$ and $\beta$, a detailed numerical summary for performance outcomes and training dynamics of an ANN model has been presented by Table 2. In the study of complex fluid dynamical profiles, it is crucial to reflect the efficiency of ANN and convergence behaviour by supporting data. For various values of $\alpha$ and $\beta$ (each set of conditions), it is clear by the table that how effectively and quickly the network adapts the accuracy. For instance, the network achieved the minimal error change at the stopping point for lower gradient values, which indicates best convergence. Whereas the smaller values of the damping parameter represent the transition of optimizer to fine-tuning from large exploration near the optimum solution. Overall, the flexibility and robustness of an artificial neural network which handles various physical situations associated with the flow has been validated through this table to ensure that the developed model is precise as well.

## 11. CONCLUSION

Here in this article blade coating analysis of non-Newtonian third order fluid has been studied. In this case the flexible blade has been used. LAT analysis has been used for the simplification of the equations. Basic governing equations are simplified using the

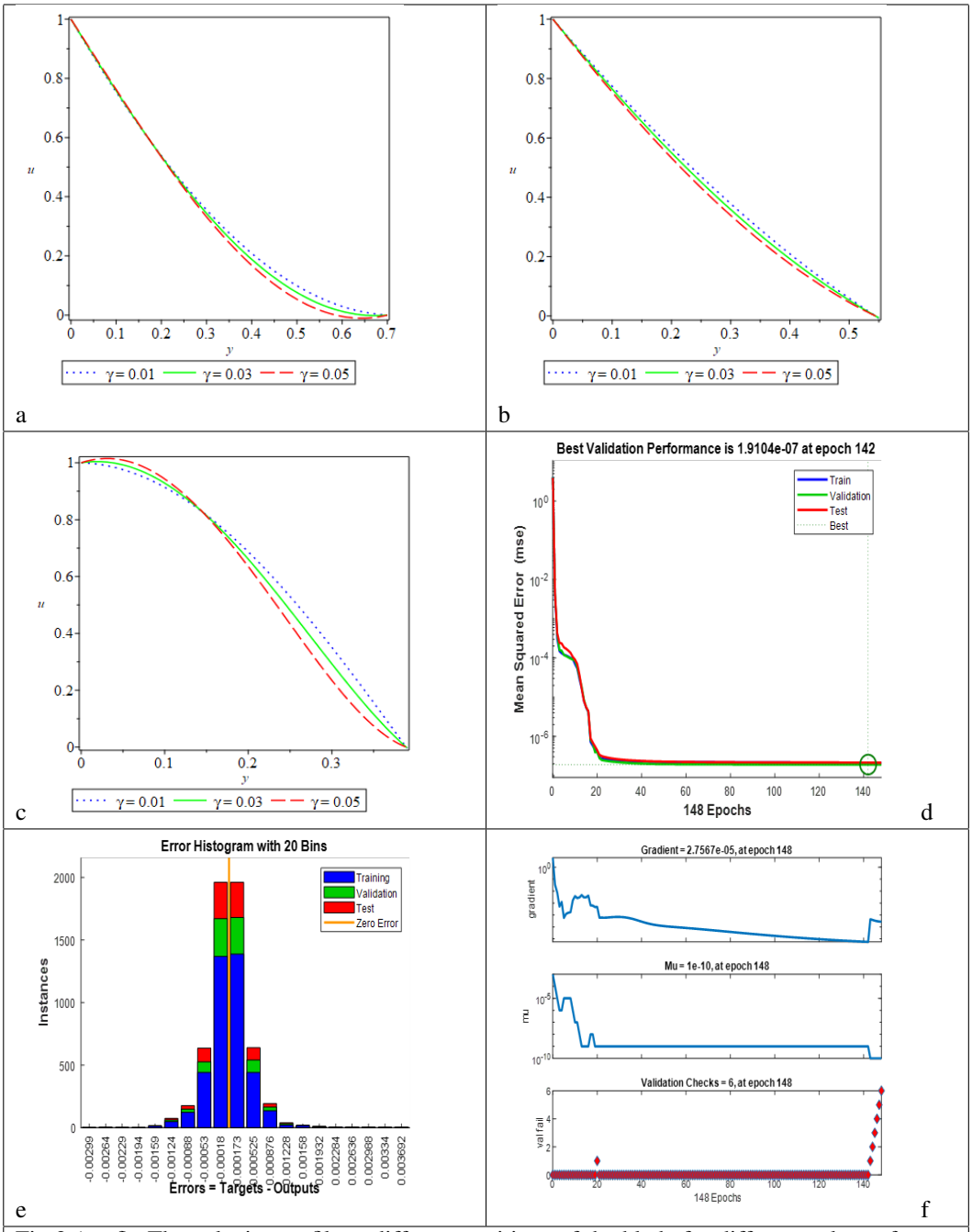


Fig 2 (a - f): The velocity profile at different positions of the blade for different values of $\gamma$, error analysis and estimation of gradient, Mu and validations checks.

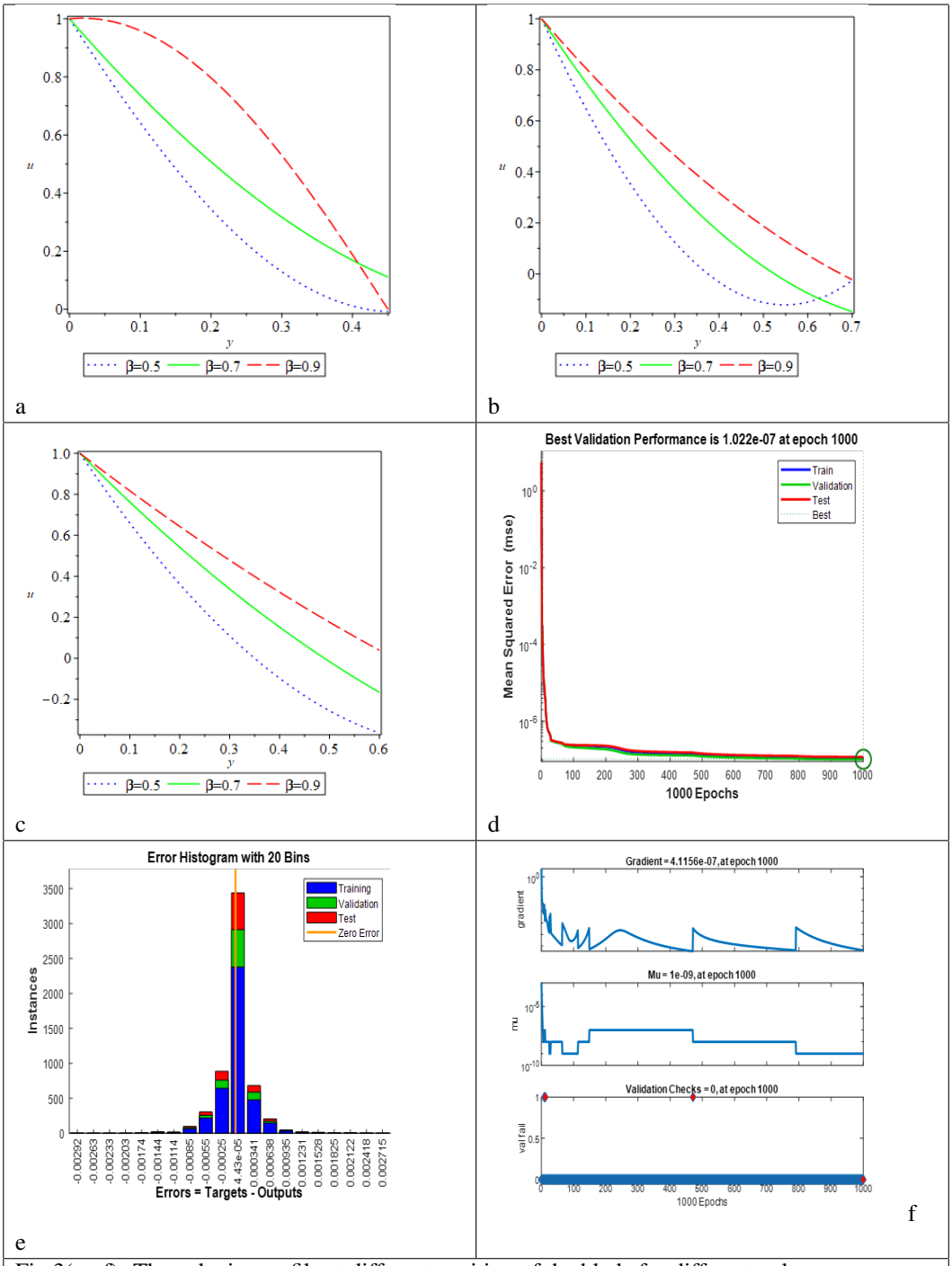


Fig 3(a - f): The velocity profile at different position of the blade for different values, error analysis and estimation of gradient, Mu and validations checks.

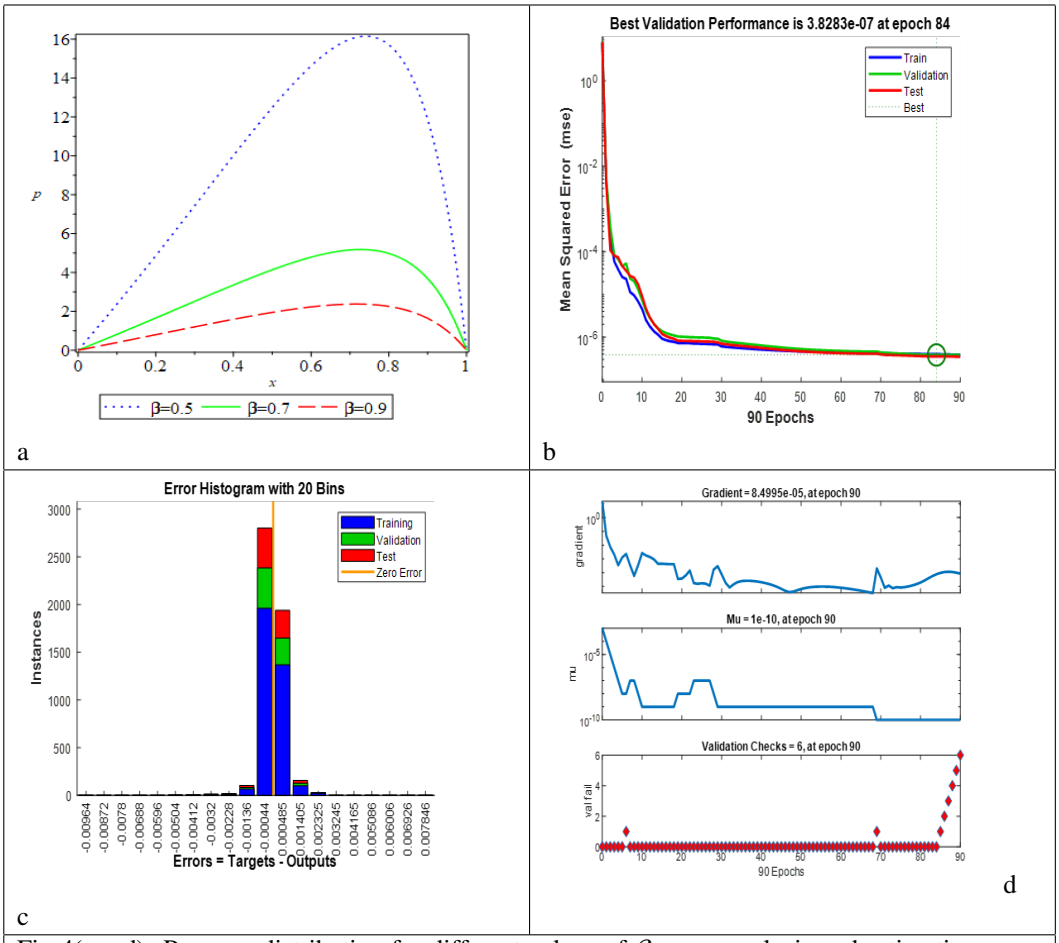


Fig 4(a – d): Pressure distribution for different values of $\beta$, error analysis and estimation of gradient, Mu and validations checks.

lubrication approximation theory. We make use of perturbation technique and numerical method for the investigation of the nature of steady state solution which exist.
The outcome of the present analysis in summarized form can be given as follows:

- Velocity of the fluid decreases by increasing the non-Newtonian parameter.
- Velocity of the fluid increases by increasing the flexibility parameter.
- Pressure increases by increasing the value of non-Newtonian parameter while it decreases by increasing the value of the flexibility parameter.
- Blade loading and coating thickness increases by increasing the value of non- Newtonian parameter.
- Blade loading decreases by increasing the value of flexibility parameter while coating thickness increases by increasing flexibility.

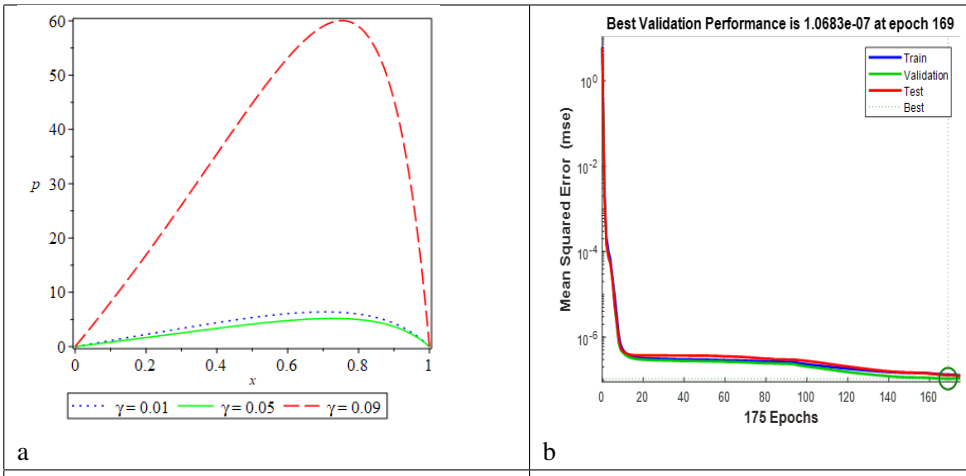


Fig 5(a - d): Pressure distribution for different values of $\gamma$, error analysis and estimation of gradient, Mu and validations checks.

The present results are more generalized than the results of Middleman [4]. By putting the value of parameter of flexibility zero results of Middleman can be retrieved. Also, previously the blade coating analysis of third order fluid has been studied [20]. Here in this work, we have considered the blade coating analysis of third order fluid with flexibility.

It is clear that coating thickness can be increases or decreases by changing the value of these parameter, it is very important from the industrial point of view. Desired thickness can be obtained by changing and controlling these parameters.

This work can be extended by using the MHD effects. Here we have used the flexible blade exponential blade can also be used. There are variety of non- Newtonian fluids in nature as in coating industries different types of fluids are used. we can also extend this work by using some other non- Newtonian fluids in the study.

TABLE 1. Numerical estimation of training, validation, performance, gradient, Mu and time for velocity profile.

| S(1) | Velocity for $\gamma = 0.01$ | | | Velocity for $\gamma = 0.03$ | | | Velocity for $\gamma = 0.05$ | | |
|---|---|---|---|---|---|---|---|---|---|
| | Initial Value | Stopped Value | Target Value | Initial Value | Stopped Value | Target Value | Initial Value | Stopped Value | Target Value |
| Epoch | 0 | 148 | 1000 | 0 | 728 | 1000 | 0 | 183 | 1000 |
| Elapsed Time | - | 00:00:02 | - | - | 00:00:08 | - | - | 00:00:02 | - |
| Performance | 4.07 | 2.13e-07 | 0 | 8.34 | 8.56e-08 | 0 | 2.26 | 9.46e-08 | 0 |
| Gradient | 6.07 | 2.76e-05 | 1e-07 | 9.13 | 6.33e-06 | 1e-07 | 3.95 | 1.59e-06 | 1e-07 |
| Mu | 0.001 | 1e-10 | 1e+10 | 0.001 | 1e-09 | 1e+10 | 0.001 | 1e-08 | 1e+10 |
| S(2) | Velocity for $\beta = 0.5$ | | | Velocity for $\beta = 0.7$ | | | Velocity for $\beta = 0.9$ | | |
| | Initial Value | Stopped Value | Target Value | Initial Value | Stopped Value | Target Value | Initial Value | Stopped Value | Target Value |
| Epoch | 0 | 1000 | 1000 | 0 | 246 | 1000 | 0 | 1000 | 1000 |
| Elapsed Time | - | 00:00:11 | - | - | 00:00:03 | - | - | 00:00:12 | - |
| Performance | 5.46 | 1.1e-07 | 0 | 7.62 | 5.59e-07 | 0 | 2.32 | 1.15e-06 | 0 |
| Gradient | 4.88 | 4.12e-07 | 1e-07 | 9.07 | 5.08e-06 | 1e-07 | 3.27 | 4.51e-06 | 1e-07 |
| Mu | 0.001 | 1e-09 | 1e+10 | 0.001 | 1e-07 | 1e+10 | 0.001 | 1e-08 | 1e+10 |

## AUTHOR CONTRIBUTIONS

Conceptualization, Saira Bhatti and Hafiz Abdul Wahab; methodology, Saira Bhatti and Muhammad Zahid; software, Assad Ayub and Hafiz Abdul Wahab; validation, Assad Ayub and Hunniya Sabir and Saira Bhatti; formal analysis, Assad Ayub; investigation, Assad Ayub and Saira Bhatti; data curation, Hunniya Sabir; writing-original draft preparation, Hafiz Abdul Wahab and Hunniya Sabir; writing-review and editing, Hafiz Abdul Wahab and Saira Bhatti; visualization, Assad Ayub and Muhammad Zahid. All authors have read and agreed to the published version of the manuscript.

## ACKNOWLEDGEMENTS

The authors would like to thank anonymous reviewers for their careful assessment and useful suggestions that helped us to improve the manuscript.

## CONFLICT OF INTEREST

The authors declare no conflict of interest.

TABLE 2. Numerical estimation of training, validation, performance, gradient, Mu and time for pressure distribution profile.

| S(1) | Pressure distribution for $\gamma$ = 0.01 | | | Pressure distribution for $\gamma$ = 0.05 | | | Pressure distribution for $\gamma$ = 0.09 | | |
|---|---|---|---|---|---|---|---|---|---|
| | Initial Value | Stopped Value | Target Value | Initial Value | Stopped Value | Target Value | Initial Value | Stopped Value | Target Value |
| Epoch | 0 | 175 | 1000 | 0 | 968 | 1000 | 0 | 64 | 1000 |
| Elapsed Time | - | 00:00:02 | - | - | 00:00:10 | - | - | 00:00:01 | - |
| Performance | 6.24 | 1.27e-07 | 0 | 18.5 | 7.21e-08 | 0 | 4.96 | 3e-07 | 0 |
| Gradient | 13.2 | 6.33e-06 | 1e-07 | 28.7 | 8.82e-06 | 1e-07 | 9.94 | 0.000106 | 1e-07 |
| Mu | 0.001 | 1e-08 | 1e+10 | 0.001 | 1e-10 | 1e+10 | 0.001 | 1e-09 | 1e+10 |
| S(2) | Pressure distribution for $\beta$ = 0.5 | | | Pressure distribution for $\beta$ = 0.7 | | | Pressure distribution for $\beta$ = 0.9 | | |
| | Initial Value | Stopped Value | Target Value | Initial Value | Stopped Value | Target Value | Initial Value | Stopped Value | Target Value |
| Epoch | 0 | 421 | 1000 | 0 | 90 | 1000 | 0 | 120 | 1000 |
| Elapsed Time | - | 00:00:04 | - | - | 00:00:01 | - | - | 00:00:01 | - |
| Performance | 3.29 | 2.81e-07 | 0 | 7.61 | 3.87e-07 | 0 | 11.3 | 3.58e-07 | 0 |
| Gradient | 7.86 | 9.07e-07 | 1e-07 | 14.9 | 8.5e-05 | 1e-07 | 17.9 | 1.15e-05 | 1e-07 |
| Mu | 0.001 | 1e-08 | 1e+10 | 0.001 | 1e-10 | 1e+10 | 0.001 | 1e-10 | 1e+10 |

TABLE 3. Tabular form of results

| $\gamma$ | $\lambda$ | L |
|---|---|---|
| 0.001 | 0.72854 | 4.045500 |
| 0.002 | 0.74524 | 4.046500 |
| 0.003 | 0.76931 | 4.047500 |
| 0.004 | 0.78442 | 4.048500 |
| 0.005 | 0.80241 | 4.049500 |
| 0.006 | 0.82433 | 4.050500 |
| 0.007 | 0.84311 | 4.051500 |
| 0.008 | 0.86243 | 4.052500 |
| 0.009 | 0.88753 | 4.053500 |

TABLE 4. Tabular form of results

| $\beta$ | $\lambda$ | L |
|---|---|---|
| 0.2 | 0.00421 | 64.713010 |
| 0.4 | 0.00532 | 16.1790026 |
| 0.6 | 0.00584 | 7.191223 |
| 0.8 | 0.00657 | 4.045500 |
| 1 | 0.00758 | 2.589480 |

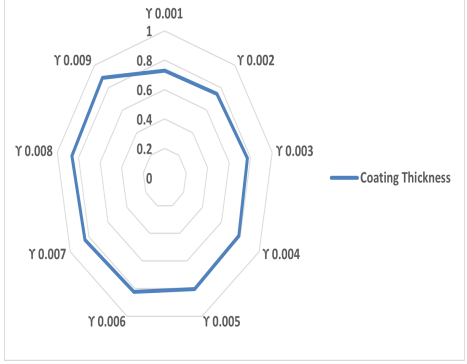


6

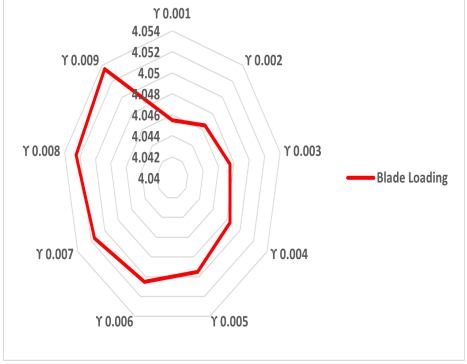


7

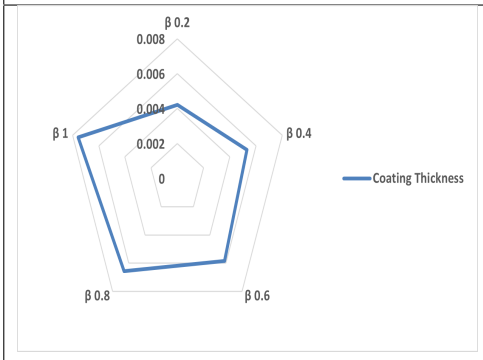


8

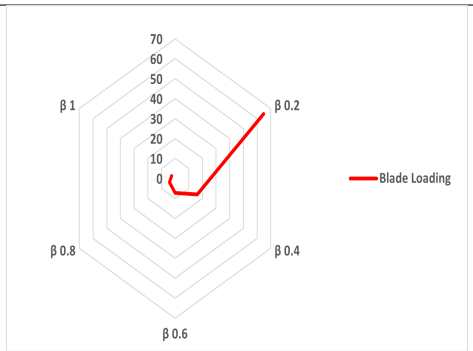


9

Figure (6 - 9): Statistical graphs of physical analysis of numerical values tabulated in Table 4 and Table 5.

## REFERENCES


[1] N. Ali, H. M. Atif, and M. A. Javed, *A theoretical analysis of roll-over-web coating of couple stress fluid*, J. Plast. Film Sheet **34** (2018): 43-59.

[2] S. Bhatti, M. Zahid, M. A. Rana, A. M. Siddiqui, and H. A.Wahab, *Numerical analysis of blade coating of a third order fluid*, J. Plast. Film Sheet 35 (2019):157-180.

[3] G. L. Booth, *Coating equipment and processes*, Lockwood Publishing Co. Inc., New York, (1970).

[4] P. Bourgin, (ed.), T. D. Blake, and Y. D. Shikhmurzaev, The moving contact line problem in coating flows: Experiments and theoretical approaches. The Second European Coating Symp. (EUROMECH 367) on Fluid Mechanics of Coating Processes, Strasbourg, France, July 22-25, (1997): 134-135.

[5] C. M. Corvalan, and F. A. Saita, *Blade coating on a compressible substrate*, Chem. Eng. Sci *50* (1995): 1769-1783.

[6] I. K. Dien, and H. G. Elrod, A *generalized steady-state Reynolds equation for non- Newtonian fluids, with application to journal bearings*, J. Lubr. Tech. (ASM International) **105**, (1983): 385.

[7] M. Fenol, E. T. Dolapc, Y. Aksoy, and M. Pakdemirli, *Perturbation-iteration method for first-order differential equations and systems*, Abstr. Appl. Anal. **2013** (2013): 1-6.

[8] P. H. Gaskell, M. D. Savage, and J. L. Summers, *1st European coating symposium on the mechanics of thin film coatings, Leeds University, UK*, 19-22 September (1995): 288-297.

[9] A. J. Giacomi, J. D. Cook, L. M. Johnson, and A. W. Mix, *Flexible Blade Coating*, J. Coat. Technol. Res. **9**, No. 3 (2012): 269-277.

[10] Y. Greener, and S. Middleman, *Blade coating of a viscoelastic fluid*, Poly. Eng. Sci. **14** (1974): 791-796.

[11] T. C. Hsu, M. Malone, and R. L. Laurence, *Separating forces in blade coating of viscous and viscoelastic liquids*, J. Non-Newton. Fluid Mech. **18** (1985): 273-294.

[12] S. S. Hwang, *Non-Newtonian liquid blade coating process*, J. Fluids Engg. **104**, (1982): 469- 475.

[13] M. Krapez, A. Gauthier, H. Kellay, J. B. Boitte, O. Aubrun, J. Joanny, and A. Colin, *Impact of the wetting length on flexible blade spreading*, Phys. Rev. Lett. **125** (2020): 254506.

[14] S. Middleman, Fundamentals of polymer processing, McGraw-Hill College, New York, (1977).

[15] M. A. Rana, A. M. Siddiqui, S. Bhatti and M. Zahid, *The study of the blade coating process lubricated with Powell-Eyring fluid*, J. Nanofluids **7** (2018): 110.

[16] A. B. Ross, S.K. Wilson, and B. R. Duffy , *Blade coating of a power law fluid*, Phy. of Fluids **11** (1999): 958-970.

[17] K. J. Ruschak, *Coating flows*, Ann. Rev. of Fluid Mech. **17** (1985): 65-89.

[18] M. Sajid, H. Shahzad, and M. Mughees, *Mathematical modeling of slip and magneto-hydrodynamics effects in blade coating*, J. Plast. Film Sheet **35** (2019): 9- 21.

[19] M. D. Savage, *Variable speed coating with purely viscous Non-Newtonian fluids*, Z. Angew. Math. Phys. **34** (1983): 358.

[20] P. M. Schweizer and S. F. Kistler, *Liquid Film Coating: Scientific principles and their technological implications*, 1st Edition, Chapman & Hall, London, (1997).

[21] A. M. Siddiqui, S. Bhatti, M. A. Rana, and M. Zahid, *Blade coating analysis of a Williamson fluid*, Results Phys. **7** (2017): 2845-2850.

[22] P. Sinha, and C. Singh, *Lubrication of a cylinder on a plane with a non-Newtonian fluid considering cavitation*, J. of Lub. Tech. **104** ( 1982): 168.

[23] J. A. Tichy, *Non-Newtonian lubrication with the convected Maxwell model*, J. Tribol **118** (1996): 344-348.

[24] B. M. Villegas-Martinez, F. Soto-Eguibar, H. M. Moya-Cessa, *Application of perturbation theory to a master equation*, Abstr. Appl. Anal. **2016** (2016): 1-7.

[25] X. Wang, H. Shahzad, Y. Chen, M. Kanwal, and Z. Ullah, *Mathematical modelling for flexible blade coater with magnetohydrodynamic and slip effects in blade coating process*, J. Plast. Film Sheet **36** No. 1 (2019): 38-54.

[26] R.W. Zimmerman, S. Kumar, and G. S. Bodvarsson, *Lubrication theory analysis of the permeability of rough-walled fractures*, nt. J. Rock Mech. Min. Sci. Geomech. Abstr. **28** No. 4 (1991): 325-331.